Computer simulation of self-assembling processes of a binary mixture containing a block copolymer

Toshihiro Kawakatsu*
Department of Physics, Faculty of Science, Kyushu University 33, Fukuoka 812, Japan
(Received 26 April 1994)

We propose a continuum model for phase separating binary mixtures containing an amphiphilic block copolymer that serves as a surfactant. The model is an extension of a recent density functional theory for block copolymer melts, and the model takes the intramolecular structure of the block copolymer molecule (surfactant molecule) in an averaged sense. We show results of a computer simulation on this model, and discuss the important contributions from the intramolecular structure of the surfactant to the phase separation dynamics, which have usually been neglected in the recent simulations on the phase separation of surfactant solutions that use continuum descriptions.

PACS number(s): 36.20.−r, 64.60.Cn, 82.70.Kj

I. INTRODUCTION

A rich variety of self-assembling supermolecular structures of surfactant solutions have been attracting the attention of physicists, chemists, and engineers [1,2]. So far, most of the investigations have been focused on the static aspects of these self-assembling structures. In a series of recent works [3–5], we explored a dynamical model, which is called *a hybrid model,* for the surfactant solutions, where the intramolecular structure of the surfactant molecule is explicitly taken into account by combining a continuum description and a molecular description. In this hybrid model, the degree of freedom of the solvent is coarse grained, while the surfactant is treated as discrete molecules.

The aim of the present paper is to propose another simplified dynamical model, where the coarse-graining procedure is also adopted to the surfactant, and therefore the model is described by fully continuum descriptions. Although there exist several continuum models for surfactant solutions using Ginzburg-Landau expansions [6–8], intramolecular structures of the surfactant molecule were totally neglected [6] or incorporated only partially through a director field of the surfactant molecules [7,8]. Such treatments are valid as long as the surfactant molecule is small compared with the characteristic length (for example, average domain size or the correlation length of the composition fluctuation) of the binary mixture. However, if the surfactant molecule is so large as to be comparable or greater than the characteristic length of the binary mixture, more detailed information on the intramolecular structure should be taken into account. This is the case for an amphiphilic block copolymer. For a block copolymer with a sufficiently large polymerization index (>1000 and $\sim 10\,000$), its gyration radius can be of the order of $10\sim 100$ Å, which is much greater than the molecular scale.

A well known approach to investigating microphase separating block copolymers is the density functional (DF) approach [9–13]. In the DF approach, the chain conformation of the block copolymer is described by a monomer density distribution function, and the total free energy of the system is given as a functional of such a monomer density distribution function. Leibler explored a DF theory for the microphase separating block copolymer melts near the critical point (weak segregation regime) [9], while the same approach was also successfully applied to microphase separations well inside the coexisting region (strong segregation regime) [10–12]. Recently, such DF approaches were used to investigate the formation and dynamics of microphase separated structures of block copolymer melts [13]. In these DF approaches, the chain conformation and the composition of the block copolymer chain are taken into account in an averaged sense. In this paper, we combine the time dependent Ginzburg-Landau (TDGL) model with the DF description of block copolymer melts in order to investigate self-assembling processes of binary mixtures containing block copolymers.

II. MODEL

Our model is a simple extension of the DF theory for block copolymer melts [9–13]. A naive description of our model has already been described in our recent paper [14]. Here we present a detailed derivation of the model. For simplicity, we consider a simple case of an A/B binary mixture containing an A-B type block copolymer, where the A monomer and the B monomer of the block copolymer are assumed to be the same as the A molecule and the B molecule of the binary mixture, respectively [14]. In general, a C-D type block copolymer serves as a surfactant in an A/B binary mixture, when the C and the D monomers are chemically similar to the A and the B molecules of the binary mixture [12]. An extension of the present model to such a general situation is straightforward.

Let us denote the number densities of the A molecules and the B molecules of the binary mixture at position $\mathbf{r}$ as $\phi_A(\mathbf{r})$ and $\phi_B(\mathbf{r})$, and those for the A monomers and the B monomers of the block copolymer as $\psi_A(\mathbf{r})$ and $\psi_B(\mathbf{r})$. As we are interested in the formation process of self-assembling structures, whose time scale is much longer than that of the sound waves, the mixture can be regard-

*Permanent address: Department of Physics, Tokyo Metropolitan University, Hachioji, Tokyo 192-03, Japan.

ed as incompressible. Assuming that the molecular volumes of the A monomer and the B monomer are equal, the incompressibility condition can be expressed as

$$\phi_A(\mathbf{r})+\phi_B(\mathbf{r})+\psi_A(\mathbf{r})+\psi_B(\mathbf{r})\equiv\rho_0 , \tag{2.1}$$

where ρ_0 is the total monomer number density. The relevant order parameters for the system are

$$\begin{aligned} &X(\mathbf{r})\equiv\phi_A(\mathbf{r})-\phi_B(\mathbf{r}) , \quad Y(\mathbf{r})\equiv\psi_A(\mathbf{r})-\psi_B(\mathbf{r}) , \\ &\phi(\mathbf{r})\equiv\phi_A(\mathbf{r})+\phi_B(\mathbf{r}) , \quad \psi(\mathbf{r})\equiv\psi_A(\mathbf{r})+\psi_B(\mathbf{r}) . \end{aligned} \tag{2.2}$$

The incompressibility condition, Eq. (2.1), leads to the fact that only three of these order parameters are independent. We choose X, Y, and ψ as the independent parameters.

The total free energy functional F is divided into the short range part F_S and the long range part F_L [11,13]. Using a cubic lattice model, the short range part is expressed by the following free energy functional (see the Appendix) [14,15]:

$$\begin{aligned} F_S=\frac{k_BT}{2\rho_0}\int d\mathbf{r}\Big\{ &-\frac{z\chi}{2}(X+Y)^2+\frac{a^2\chi}{2}|\nabla(X+Y)|^2 \\ &+\rho_0[(\phi+X)\ln(\phi+X)+(\phi-X)\ln(\phi-X) \\ &+(\psi+Y)\ln(\psi+Y)+(\psi-Y)\ln(\psi-Y)]\Big\} \\ &+\text{ constant contributions} , \end{aligned} \tag{2.3}$$

where k_B is the Boltzmann constant, T is the temperature, z is the total number of the nearest neighbor sites on the lattice ($z=6$ for cubic lattice), $a\equiv\rho_0^{-1/3}$, and χ is the usual χ parameter defined by

$$\chi\equiv\chi_{AB}-\tfrac{1}{2}(\chi_{AA}+\chi_{BB}) , \tag{2.4}$$

χ_{AA}, χ_{BB}, and χ_{AB} being the interaction energy between A-A, B-B, and A-B nearest neighbor pairs divided by k_BT. The constant contributions to the free energy in Eq. (2.3) arise due to the conservation laws for the fields X, Y, ϕ, and ψ, and these contributions do not play any role in the dynamics.

The long range part F_L originates from the conformational entropy of the block copolymer chain. As the A block and the B block of a block copolymer chain are connected by a chemical bond, a macrophase separation is inhibited for the block copolymer. Such a character imposes a penalty on the long wavelength fluctuations in the field $Y(\mathbf{r})$. Following Ohta and Kawasaki [11], we write this penalty as

$$F_L=\alpha\int d\mathbf{r}\,d\mathbf{r}'G(\mathbf{r}-\mathbf{r}')[Y(\mathbf{r})-\bar{Y}][Y(\mathbf{r}')-\bar{Y}] , \tag{2.5}$$

where $G(\mathbf{r})$ satisfies $\nabla^2G(\mathbf{r})=-\delta(\mathbf{r})$, $\bar{Y}$ is the spatial average of $Y(\mathbf{r})$, and α is a positive constant. Fourier transformation of Eq. (2.5) leads to $F_L\sim\alpha\sum(1/k^2)|Y_{\mathbf{k}}|^2$, and therefore this free energy imposes a penalty on the long wavelength fluctuations in $Y(\mathbf{r})$. Since the long wavelength composition fluctuation should be suppressed especially for shorter block copolymer chains, the penalty coefficient α increases as N decreases. More precisely, it is known that α depends on the polymerization index N of the block copolymer chain as $\alpha\sim N^{-2}$ [11].

For the dynamics, we adopt the purely dissipative dynamics as is done for the usual TDGL model:

$$\frac{\partial X}{\partial t}=L^X\nabla^2\frac{\delta F}{\delta X} , \tag{2.6}$$

where $F=F_S+F_L$. We assume similar equations of motion for $Y(\mathbf{r},t)$ and $\psi(\mathbf{r},t)$. In Eq. (2.6), we neglected the cross coupling currents between different order parameters and the thermal fluctuation effects. The hydrodynamic interaction, which is also neglected in Eq. (2.6), becomes important in the later stage, as is actually observed in the real experiments using polymer blends and block copolymers [16]. Within a certain time regime (in the early stage), one can neglect such a hydrodynamic interaction. A simple order estimate of the characteristic time scales associated with the present system is given in our previous work [5].

III. NUMERICAL SIMULATION

We performed a numerical simulation based on the model presented in the preceding section. As the logarithmic functions in the free energy expression Eq. (2.3) are highly nonlinear functions, the equations of motion are stiff differential equations, which are not suitable for numerical simulations. In order to avoid this difficulty, we expand Eq. (2.3) in a power series of the order parameters (the so-called Ginzburg-Landau expansion). Such an expansion is justified when the system is in the vicinity of the critical point, where the amplitudes of the fluctuations are small. We also add a term $|\nabla\psi|^2$ to Eq. (2.3) that is irrelevant to the physical properties but improves the stability of the numerical scheme. The details of the expansion procedure are given in the Appendix.

Numerical simulations from initial random distribution of the three-component mixture were performed. The system is a two-dimensional square box, which is divided into 128×128 meshes with a mesh width 1.0. We impose periodic boundary conditions on each box side. The initial configurations of the fields $X(\mathbf{r})$, $Y(\mathbf{r})$, and $\psi(\mathbf{r})$ at each mesh point were generated using Gaussian random numbers with mean values $\bar{X}$, $\bar{Y}$, and $\bar{\psi}$ and the values of variance 0.04^2, 0.04^2, and 0.04, respectively. We choose the parameters as $\tilde{L}^Y=\tilde{L}^\psi=1.0$, $\bar{X}=0.0$ (symmetric composition of the binary solvent), $\bar{Y}=0.0$ (symmetric block copolymer case), $\bar{\psi}=0.2$ (20% block copolymer volume fraction), the coefficient of the term $|\nabla\psi|^2$ as 1.0, and $z=6$ and $\chi=0.5$, respectively. The equations of motion, Eqs. (A4), were integrated numerically using the standard Euler scheme with a time mesh $\Delta t=0.005$ up to 400 000 steps ($t=2000.0$). We performed a series of simulation runs, changing the value of α as $\alpha=0.0$, 0.1, 0.2, 0.5, 1.0, 2.0, 5.0, and 10.0, keeping the other parameters constant. This corresponds to changing the polymerization index of the block copolymer chains, keeping the total volume fraction of the block copolymer constant. In the following, all the data shown are averaged over five independent runs using different initial configurations.

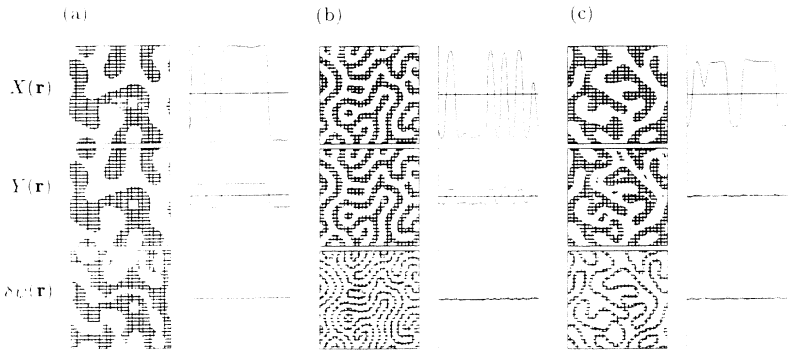

FIG. 1. Snapshots of the fields $X(\mathbf{r},t)$, $Y(\mathbf{r},t)$, and $\delta\psi(\mathbf{r},t)$ at $t=2000.0$ are shown for the cases with (a) $\alpha=0.0$, (b) $\alpha=1.0$, and (c) $\alpha=10.0$, respectively. The left-hand and the right-hand figures show the configuration of the fields and the cross-section profiles of the fields, respectively.

In Fig. 1, snapshots of the fields $X(\mathbf{r},t)$, $Y(\mathbf{r},t)$, and $\delta\psi(\mathbf{r},t)\equiv\psi(\mathbf{r},t)-\bar{\psi}$ at $t=2000.0$ are shown for the cases with (a) $\alpha=0.0$, (b) $\alpha=1.0$, and (c) $\alpha=10.0$, respectively. In each case, the left-hand figures show the configurations of the fields, where the regions with positive field values are shaded. The right-hand figures are the cross-section profiles of the fields along the horizontal line that passes the center of the box. The case (a) is identical to a phase separating A/B binary mixture because there is no long range interaction coming from the chain connectivity. On the other hand, the polymer effect is important in cases (b) and (c). In case (b), a clear domain structure, which resembles that of the microphase separating block copolymer melt [13], is formed for the fields X and Y. The domain structure in case (c) has a somewhat intermediate nature between the two cases (a) and (b), which suggests that the polymer nature becomes less important for short block copolymer chains (note that α is a decreasing function of the chain length). In cases (b) and (c), the distribution of $\delta\psi$ shows that the block copolymer is accumulated at interfaces between domains, which is expected from the surfactant nature of the amphiphilic block copolymer.

Scattering structure functions for the fields X and Y, denoted as $S_X(k,t)$ and $S_Y(k,t)$, are defined as

$$S_X(k,t)\equiv|X_{\mathbf{k}}(t)|^2\ ,\quad S_Y(k,t)\equiv|Y_{\mathbf{k}}(t)|^2\ , \tag{3.1}$$

where $X_{\mathbf{k}}(t)$ and $Y_{\mathbf{k}}(t)$ are the Fourier components of $X(\mathbf{r},t)$ and $Y(\mathbf{r},t)$ with the wave vector $\mathbf{k}$. In Figs. 2 and 3, we show temporal changes of the characteristic wave numbers $\langle k_X(t)\rangle$ and $\langle k_Y(t)\rangle$, which are defined as the first moments of $S_X(k,t)$ and $S_Y(k,t)$ [5] for various values of α. Note that the characteristic lengths of the spatial patterns of $X(\mathbf{r},t)$ and $Y(\mathbf{r},t)$ are inversely proportional to these characteristic wave numbers.

Figure 2 shows the data for the cases with smaller values of α, i.e., for longer block copolymers. One finds that the two characteristic wavelengths $\langle k_X\rangle$ and $\langle k_Y\rangle$ behave in almost the same manner. There is no penalty for the macrophase separation for the case with $\alpha=0.0$, and both characteristic wave numbers $\langle k_X\rangle$ and $\langle k_Y\rangle$ continue to decrease as $t^{-1/3}$, like the phase separating simple binary mixture without hydrodynamic effects [17]. As α increases (the length of the block copolymer chain decreases), the phase separation is more and more slowed down, and finally the domain structures are almost frozen. The final domain structures become more and more fine grained as α is increased. Such a feature is well known for microphase separating block copolymer melts [9–11,13]. Therefore, the final domain structures in these cases are dominated by the phase separation of the block copolymers, just like the case where selected solvents are solvated into microphase separating block copolymer melts [18]. One can also observe that the domain structure in the early stage becomes more fine grained as the chain length of the block copolymer is decreased (α is increased). This tendency shows that the phase separation at the initial stage is affected by the intramolecular structure of the block copolymer chain, as we pointed out in our previous works [4,5].

The behavior of the characteristic wavelengths changes

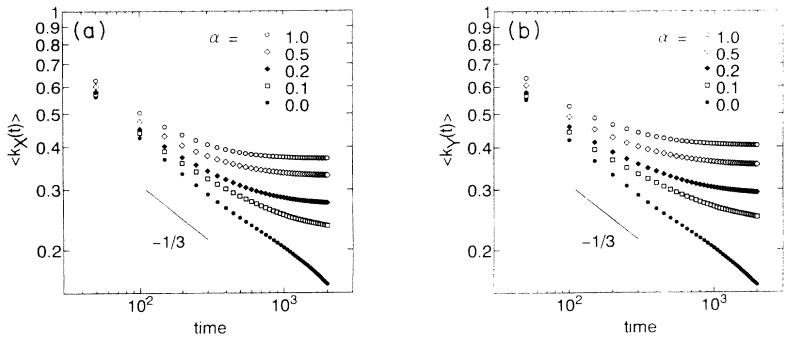

FIG. 2. Temporal changes of the characteristic wave numbers (a) $\langle k_X(t)\rangle$ and (b) $\langle k_Y(t)\rangle$ for $\alpha\leq 1.0$.

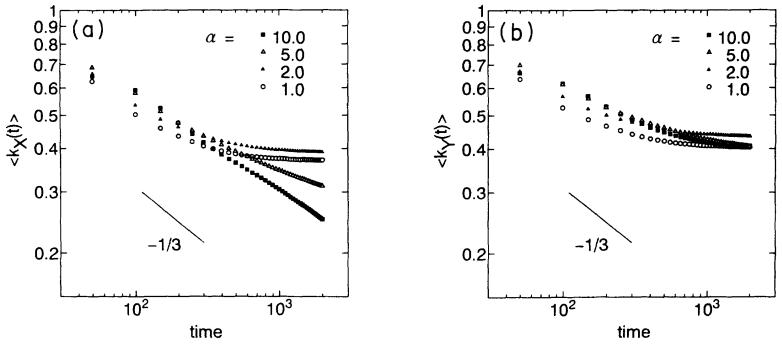

FIG. 3. Same as Fig. 2, but for $\alpha \geq 1.0$.

qualitatively for $\alpha > 1.0$ (short block copolymer chains), which are shown in Fig. 3. In this region, the phase separation for the field X [Fig. 3(a)] is not frozen by the block copolymer within the same time range for the domain freezing for the cases shown in Fig. 2. Contrary to such behavior, one verifies in Fig. 3(b) that the temporal change in the characteristic wave number for the field Y is almost frozen in the late stage. This means that the microphase separation of the block copolymer no longer dominates the entire phase separation due to the insufficient length of the block copolymer chain. One can, however, still observe a slight slowing down of the phase separation for the field X in the late stage, which should be attributed to the surfactant nature of the amphiphilic block copolymer [5,6]. As is theoretically known, the surfactant property becomes small for shorter block copolymer chains [12]. Therefore, the slowing down of the phase separation becomes less noticeable for the shortest block copolymer case ($\alpha = 10.0$).

In order to confirm that the phase separation is dominated by the microphase separation of the block copolymer for $\alpha < 1.0$, we plotted in Fig. 4 the values of the characteristic wave numbers $\langle k_X(t) \rangle$ and $\langle k_Y(t) \rangle$ at $t = 2000.0$ ($\equiv t_0$) in a double logarithmic plot. As is observed in Fig. 2, the domain structures are almost frozen at this time for $0.1 \leq \alpha \leq 1.0$. Within such a parameter range, we observe a power law dependence $\langle k(t_0) \rangle \sim \alpha^{\theta}$, with $\theta \sim \frac{1}{4}$. Such a power law dependence is actually expected for microphase separating block copolymers in the weak segregation regime [9,13]. In the weak segregation regime, the domain size is known to be proportional to $N^{1/2}$, N being the chain length of the block copolymer.

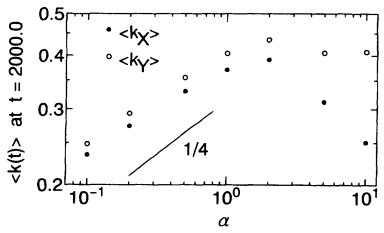

FIG. 4. The values of the characteristic wave numbers $\langle k_X(t) \rangle$ and $\langle k_Y(t) \rangle$ at $t = 2000.0$ are shown as functions of α.

Combining this relation with $\alpha \sim N^{-2}$, one obtains the relation $\langle k(t_0) \rangle \sim \alpha^{1/4}$. Therefore, this result shows that the final domain structures are maintained by the block copolymers for $\alpha < 1.0$.

Next, we discuss the changes in the domain morphology. In order to discuss the domain morphology quantitatively, we calculated the scaled scattering function $\tilde{S}_X(x)$, defined by

$$S_X(k,t) = \langle k_X(t) \rangle^{-d} \tilde{S}_X[k / \langle k_X(t) \rangle] , \tag{3.2}$$

where d is the spatial dimension [5]. In Fig. 5, we show the scaled scattering function $\tilde{S}_X(x)$ in double logarithmic plots for the cases (a) $\alpha = 0.0$, (b) $\alpha = 1.0$, and (c) $\alpha = 10.0$, respectively. In order to eliminate the finite size effects of the simulation system, these scaled scattering functions are obtained at (a) $t = 100.0$, (b) $t = 250.0$, and (c) $t = 300.0$, when the domain structures for the respec-

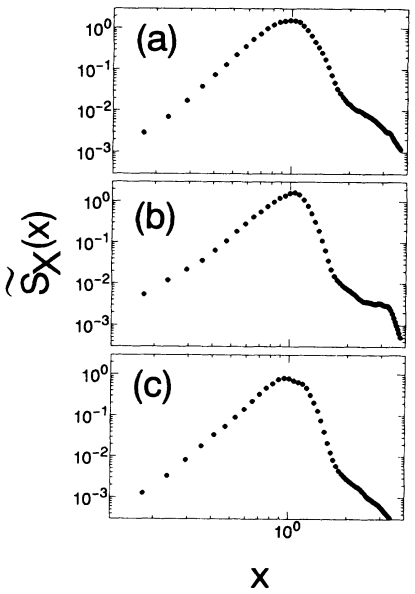

FIG. 5. The scaled scattering function $\tilde{S}_X(x)$ for the cases (a) $\alpha = 0.0$, (b) $\alpha = 1.0$, and (c) $\alpha = 10.0$ in double logarithmic plots. These data are obtained at (a) $t = 100.0$, (b) $t = 250.0$, and (c) $t = 300.0$, respectively, when these domain structures have almost the same characteristic wave number.

tive cases have almost the same characteristic wave numbers (see Figs. 2 and 3). Case (a) corresponds to the characteristic scaled scattering function for a phase separating binary mixture, which has a main peak at $x=1$ and has a shoulder at $x\sim 3$, the latter shoulder originating from the local lamellar ordering of the domains. Such a shoulder becomes much more pronounced in case (b) and the main peak becomes sharper than in case (a). This confirms our speculation that the domain structure is dominated by the microphase separation of the block copolymer, which leads to a lamellar structure in the present symmetric block copolymer case. The scaled scattering function in case (c) resembles that in case (a), which means that the phase separation in this case is dominated not by the microphase separation of the block copolymer, but by the phase separation of the binary solvent.

In our previous simulation, using another model called *the hybrid model* [5], we reported that the main peak of the scaled scattering function becomes broader when we add a surfactant into a binary solvent mixture. Such a main peak broadening was attributed to the undulation of the interfaces caused by a buckling of the surfactant sheets on the interfaces. This apparently contradicts the results shown in Figs. 5(a) and 5(b), where the main peak becomes sharper when adding the block copolymer. However, the phase separation was obviously dominated by the binary solvent in Ref. [5]. Therefore, we should compare the results in Ref. [5] with those in Figs. 5(a) and 5(c), where there is very little difference in the main peak width. This is due to the fact that the phase separation has not proceeded enough to produce the interfacial undulation in Fig. 5(c).

Actually, a broadening of the main peak can also be observed in the present simulation at later times. In Fig. 6(a), we show a comparison of the scaled scattering functions $\tilde{S}_X(x)$ for the two cases $\alpha=0.0$ and $\alpha=10.0$, calculated in the later time stage than those in Fig. 5. Here again, the times are chosen so that the characteristic wave numbers of the two domain structures have almost the same value. One finds an obvious broadening of the main peak for the case with $\alpha=10.0$, as was predicted in our earlier simulation [5]. We also show in Fig. 6(b) the scaled scattering functions $\tilde{S}_{X+Y}(x)$ for the total monomer concentration difference, including monomers of the block copolymer, $X(\mathbf{r})+Y(\mathbf{r})$, for the same domain structures as in Fig. 6(a). One can still observe the main peak broadening in Fig. 6(b), which means that the main peak broadening originates from an irregularity in the domain shape and not from some irregularities in the interfacial structure caused by the adsorbed block copolymers. A sample domain structure for the case with $\alpha=10.0$ is given in Fig. 1(c). One can easily understand that the interface undulation is the origin of such a main peak broadening. It will be worth noting that in real neutron scattering experiments, the scattering data that correspond to those in Fig. 6(a) can be obtained by using selectively deuterated samples, while the data corresponding to Fig. 6(b) can be obtained using normal protonated samples.

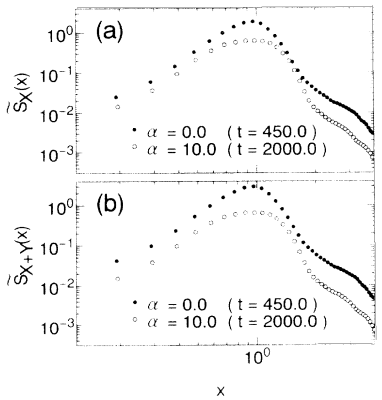

FIG. 6. A comparison of the scaled scattering functions between the two cases $\alpha=0.0$ and $\alpha=10.0$ at a later time than those in Fig. 5. (a) Scattering functions from the field $X(\mathbf{r})$ (selective scattering from the solvent) and (b) scattering function from the field $X(\mathbf{r})+Y(\mathbf{r})$ (total scattering from the sample) are shown, respectively. These scattering functions are calculated at $t=450.0$ for $\alpha=0.0$ and at $t=2000.0$ for $\alpha=10.0$, respectively, when these domain structures have almost the same characteristic wave number.

IV. CONCLUSIONS

We proposed a dynamical model for a phase separating ternary mixture of an A solvent, a B solvent, and an A-B type block copolymer, where the intramolecular structure of the block copolymer chain is taken into account using a result from recent density functional treatment of block copolymer melts [9–13]. We found that the behavior of the phase separation is qualitatively different between the case with longer block copolymers and the case with shorter block copolymers. When the block copolymer is sufficiently long, the phase separation is dominated by the microphase separation of the block copolymer, where the scattering function has a sharp main peak compared to that for the case of simple binary mixture without the block copolymer. If the block copolymer is relatively short, the phase separation is driven by the binary solvent and the block copolymer plays the role of a surfactant, which slows down the phase separation in the late stage. In such a case, we found a broadening of the main peak of the scattering function, as was predicted in our earlier work [5].

Recently, Laradji and co-workers reported results of two types of simulations on the same problem treated in the present paper [6,19]. One is a simulation using a continuum model, which corresponds to the short chain limit ($\alpha\rightarrow\infty$) of the present model, where the intramolecular structure of the surfactant is not taken into account [6]. The other is a molecular dynamics simulation using a molecular model, where the surfactant molecule is modeled as a pair of an A monomer and a B monomer connected by a harmonic spring [19]. In these two simulations, Laradji *et al.* found qualitatively the same results as those reported in the present article. One important difference is the fact that Laradji *et al.* did not observe the broadening of the main peak of the scattering func-

tion when the surfactant is added to the binary mixture [19], which seems to contradict our finding. We expect that such a contradiction may come from the difference in the sizes of the surfactant compared to the domain size. In the present simulation and in our previous simulation [5], the chain length of the block copolymer can be of the same order as the domain size [see Figs. 1(b) and 1(c)], while Laradji *et al.* used a rather smaller surfactant molecule, which does not have a polymer nature. This point should be clarified in future studies.

The present model can also be extended to investigate the phase separations in the presence of asymmetric surfactants. We investigated such a phase separation process using *the hybrid model* [14,20], where we found a crossover phenomenon in the phase separation associated with a morphological change in the domain structure. Thus, it will be important to check using the present model whether the results of *the hybrid model* are not an artifact of its particular characteristics arising from the combination of a molecular description and a continuum description [3–5].

ACKNOWLEDGMENT

The computation was done at the computer center of the Institute of Molecular Science, Japan.

APPENDIX: DERIVATION OF THE FREE ENERGY FUNCTIONAL AND ITS GINZBURG-LANDAU EXPANSION

In this appendix, we derive the short range part of the free energy functional, Eq. (2.3), and perform a Ginzburg-Landau expansion of the total free energy functional, Eqs. (2.3) and (2.5), to derive expressions for the equations of motion used in the actual simulation.

First we derive Eq. (2.3). We assume that the system consists of monomers distributed on a cubic lattice with a lattice spacing a. The short range part of the free energy F_S comes from the interactions between monomers (denoted as E) and the entropy of the transactional degrees of freedom of the monomers (denoted as S). Using the local mean field approximation, $F_S=E-TS$ is given by [14]

$$E=\frac{k_BT}{2\rho_0}\int d\mathbf{r}[z\{\chi_{AA}\rho_A^2+\chi_{BB}\rho_B^2+2\chi_{AB}\rho_A\rho_B\} -a^2\{\chi_{AA}|\nabla\rho_A|^2+\chi_{BB}|\nabla\rho_B|^2+2\chi_{AB}\nabla\rho_A\cdot\nabla\rho_B\}] , \tag{A1}$$

$$S=-k_B\int d\mathbf{r}[\phi_A\ln\phi_A+\phi_B\ln\phi_B+\psi_A\ln\psi_A+\psi_B\ln\psi_B)] , \tag{A2}$$

where $\rho_K(\mathbf{r})\equiv\phi_K(\mathbf{r})+\psi_K(\mathbf{r})$ ($K=A$ or B), and the other variables are the same as those defined in the text. In deriving (A2), we regard the block copolymer chain as a set of free monomers apart from the long range interaction arising from the connectivity of the chain, which gives the long range part of the free energy F_L. Introducing the order parameters defined in Eqs. (2.2), Eq. (A2) can be rewritten as Eq. (2.3).

Next we perform the GL expansion. Substituting Eqs. (2.3) and (2.5) into Eq. (2.6), and rescaling the variables with the unit of length $a\chi^{1/2}$, the unit of time $2a^2\chi\rho_0/k_BTL^X$, and the unit of number density ρ_0, the equations of motion are rewritten into a dimensionless form as

$$\begin{aligned}
\frac{\partial}{\partial t}X(\mathbf{r},t)&=\nabla^2\left[-z\chi(X+Y)-\nabla^2(X+Y)+\ln\frac{\phi+X}{\phi-X}\right] ,\\
\frac{\partial}{\partial t}Y(\mathbf{r},t)&=\tilde{L}^Y\nabla^2\left[-z\chi(X+Y)-\nabla^2(X+Y)+\ln\frac{\psi+Y}{\psi-Y}\right]\\
&\quad-\tilde{L}^Y\tilde{\alpha}(Y-\bar{Y}) ,\\
\frac{\partial}{\partial t}\psi(\mathbf{r},t)&=\tilde{L}^\psi\nabla^2\ln\frac{\psi^2-Y^2}{\phi^2-X^2} ,
\end{aligned} \tag{A3}$$

where all the variables are nondimensionalized and $\tilde{L}^Y\equiv L^Y/L^X$, $\tilde{L}^\psi\equiv L^\psi/L^X$, and $\tilde{\alpha}\equiv\alpha L^X$.

Let us denote the average value of $\psi(\mathbf{r})$ as $\bar{\psi}$ and introduce a deviation of $\psi(\mathbf{r})$ from its average value as $\delta\psi$, i.e., $\delta\psi(\mathbf{r})=\psi(\mathbf{r})-\bar{\psi}$. When the system is close to the critical point, the variables X, Y, and $\delta\psi$ are small, so that the equations of motion can be expanded in power series in these variables. Then we obtain the following TDGL-type equations of motion up to the lowest relevant order:

$$\begin{aligned}
\frac{\partial}{\partial t}X&=\nabla^2\left[-z\chi(X+Y)-\nabla^2(X+Y)+\frac{2}{\bar{\phi}}\left[1+\frac{\delta\psi}{\bar{\phi}}\right]X\right.\\
&\quad\left.+\frac{2}{3\bar{\phi}^3}\left[1+3\frac{\delta\psi}{\bar{\phi}}\right]X^3\right] ,\\
\frac{\partial}{\partial t}Y&=\tilde{L}^Y\nabla^2\left[-z\chi(X+Y)-\nabla^2(X+Y)+\frac{2}{\bar{\psi}}\left[1-\frac{\delta\psi}{\bar{\psi}}\right]Y\right.\\
&\quad\left.+\frac{2}{3\bar{\psi}^3}\left[1-3\frac{\delta\psi}{\bar{\psi}}\right]Y^3\right]-\tilde{L}^Y\tilde{\alpha}(Y-\bar{Y}) ,\\
\frac{\partial}{\partial t}\delta\psi&=\tilde{L}^\psi\nabla^2\left[2\left[\frac{1}{\bar{\phi}}+\frac{1}{\bar{\psi}}\right]\delta\psi+\frac{1}{\bar{\phi}^2}\left[1+2\frac{\delta\psi}{\bar{\phi}}\right]X^2\right.\\
&\quad\left.-\frac{1}{\bar{\psi}^2}\left[1-2\frac{\delta\psi}{\bar{\psi}}\right]Y^2\right] .
\end{aligned} \tag{A4}$$

These are basic equations of motion for our model simulations [21].

In the actual numerical simulations presented in this article, a term with the form $\int d\mathbf{r}|\nabla\delta\psi|^2$ is added to the free energy F in order to make the computational scheme more stable. Such an extra term does not change the physical properties of the model.

[1] *Physics of Complex and Supermolecular Fluids,* edited by S. A. Safran and N. A. Clark (Wiley, New York, 1987).
[2] *Physics of Amphiphilic Layers,* edited by J. Meunier, D. Langevin, and N. Boccara (Springer-Verlag, Berlin, 1987).
[3] T. Kawakatsu and K. Kawasaki, Physica A **167**, 690 (1990).
[4] T. Kawakatsu and K. Kawasaki, J. Colloid Interface Sci. **145**, 413 (1991); **145**, 420 (1991).
[5] T. Kawakatsu, K. Kawasaki, M. Furusaka, H. Okabayashi, and T. Kanaya, J. Chem. Phys. **99**, 8200 (1993).
[6] M. Laradji, H. Guo, M. Grant, and M. J. Zuckermann, J. Phys. A **24**, L629 (1991); J. Phys. Condens. Matter **4**, 6715 (1992).
[7] K. Kawasaki and T. Kawakatsu, Physica A **164**, 549 (1990).
[8] K. Chen, C. Jayaprakash, R. Pandit, and W. Wenzel, Phys. Rev. Lett. **65**, 2736 (1990).
[9] L. Leibler, Macromolecules **13**, 1602 (1980).
[10] E. Helfand and Z. R. Wassermann, Macromolecules **9**, 879 (1976).
[11] T. Ohta and K. Kawasaki, Macromolecules **19**, 2621 (1986); K. Kawasaki, T. Ohta, and M. Kohrogui, *ibid.* **21**, 2972 (1988); K. Kawasaki and T. Kawakatsu, *ibid.* **23**, 4006 (1990).
[12] J. Noolandi and K. M. Hong, Macromolecules **15**, 482 (1982); T. A. Vilgis and J. Noolandi, *ibid.* **23**, 2941 (1990).
[13] M. Bahiana and Y. Oono, Phys. Rev. A **41**, 6763 (1990). See also F. Liu and N. G. Goldenfeld, *ibid.* **39**, 4805 (1989); T. Ohta, Y. Enomoto, J. L. Harden, and M. Doi, Macromolecules **26**, 4928 (1993); M. Doi, J. L. Harden, and T. Ohta, *ibid.* **26**, 4935 (1993); A. Chakrabarti and J. D. Gunton, Phys. Rev. E **47**, R792 (1993).
[14] T. Kawakatsu, K. Kawasaki, M. Furusaka, H. Okabayashi, and T. Kanaya, J. Phys. Condens. Matter **6**, 6835 (1994).
[15] The term $|\nabla(X+Y)|^2$ shows the contribution from the inhomogeneity in the monomer distribution to the monomer-monomer interaction energy. The expression is valid for binary mixtures composed of molecules with low molecular weights. If the polymer blend is used as the binary mixture, this term should be replaced by the usual de Gennes–type term
$$[a^2/36(X+Y)(1-X-Y)]|\nabla(X+Y)|^2 .$$
See, for example, P. G. de Gennes, J. Chem. Phys. **72**, 4756 (1980); K. Binder, *ibid.* **79**, 6387 (1983).
[16] T. Hashimoto and T. Izumitani, Macromolecules **26**, 3631 (1993); T. Izumitani and T. Hashimoto, *ibid.* **27**, 1744 (1994).
[17] Y. Oono and S. Puri, Phys. Rev. A **38**, 434 (1988).
[18] H. Tanaka, H. Hasegawa, and T. Hashimoto, Macromolecules **24**, 240 (1991).
[19] M. Laradji, O. G. Mouritsen, S. Toxvaerd, and M. J. Zuckermann, Phys. Rev. E **50**, 1243 (1994).
[20] T. Kawakatsu, K. Kawasaki, M. Furusaka, H. Okabayashi, and T. Kanaya (unpublished).
[21] If the system is close to the tricritical point, one needs to retain terms up to the second order of $\delta\psi$. In such a case, the model reduces in the short chain limit ($\alpha \to \infty$) to the model used in Ref. [6].

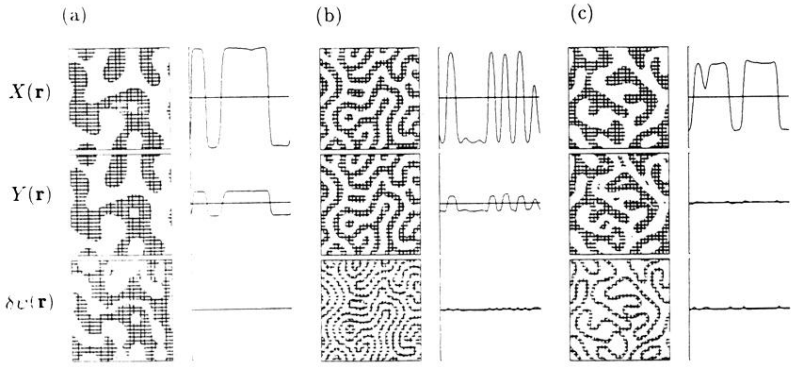

FIG. 1. Snapshots of the fields $X(\mathbf{r},t)$, $Y(\mathbf{r},t)$, and $\delta\psi(\mathbf{r},t)$ at $t=2000.0$ are shown for the cases with (a) $\alpha=0.0$, (b) $\alpha=1.0$, and (c) $\alpha=10.0$, respectively. The left-hand and the right-hand figures show the configuration of the fields and the cross-section profiles of the fields, respectively.